Turkish Online Journal of Qualitative Inquiry (TOJQI)
Volume 12, Issue 8, July 2021: 4364 – 4380

SVPWM based Bidirectional T-Type Multilevel Inverter for Electric Vehicle Applications

Dr. T.AnilKumar[1], E. AjayKumar[2]

[1]Professor,Department of Electrical and Electronics Engineering, Anurag University, Venkatapur, GhatkesarMedchal- Malkajgiri District, Telangana, India 500088
[2]PG Student, Department of Electrical and Electronics Engineering, Anurag Group of Institutions (Now Anurag University)
Email: [1]thalluruanil@gmail.com, [2]ajaykumarenamalla@gmail.com

ABSTRACT: The main aspect of this paper is SVPWM based bi-directional T-type multilevel inverter for electric vehicle applications. A multilevel dc–dc converter operates in both directions, which is required in electric vehicles. It provides additional two switches and capacitor to manage the voltage of the T-type multilevel inverter capacitor during all or at fault conditions. This arrangement of this MLI converter due to the high-cycle-by-cycle voltage balance between capacitors (CN and CP), the bulky electrolytic capacitors used in T-type MLI, are replaced with longer life film capacitors resulting in a size and weight reduction of the converter by 20 percent. This allows increased space to increase the battery capacity. In this present system, THD and line voltages have more signals. LUCC will be minimized due to the utilization of SVPWM concept.

Keywords: space vector pulse width modulation (SVPWM), T-type multilevel inverter, EV, THD.

I. INTRODUCTION

In order to address various applications [1]–[3], multi-level inverter (MLI) topologies have been implemented. In general, In order to synthesize their step by step output levels, the power source is divided from the MLIS by dc or a single-dc power source separating condenser. The first type is more stable; however, it needs increasing numbers of energy sources and power switches, like H-bridgeMLI cascades.Split condenser-based MLIs such as MLIs with neutral split condenser (NPC)[4], MLI[5] with flying condenser (FC) and MLI Form [6][7], on the other hand, need less power component amount. However, since Voltages in each capacitor are relayed in an ideal natural equilibrium, the voltages of these condensers are in practice susceptible to voltage drifting leading to to voltage imbalance. A bidirectional dc-dc transverter [8]–[10] is used for EV applications to run the inverter in propulsion system. In order to allow power from the electric machineback to power or storage units as in electrical transmission in reverse mode, the two-way transducer stepped on the DC voltage. The two-way converter comes as an immotor boost and a bump converter in failure, or vice versa, through the power supply connected to the propulsion system.

While conventional DC-DC translators for dc bus tension control are highly reliable, MLIs[11][12] are not always the relationship. As defined, a single dc power supply connected MLI is used to generate its output voltages at its sublevel as the input stage on a split condenser. This type of device is susceptible to unequaled condenser voltages and thus neutral point voltage differentiation [1]. An additional circuitry must be added to ensure the condensers' equilibrated voltage and stabilize the neutral point [13], or without the control loop, [14]. Another approach is to use a changed scheme [15] that opts for restoring the voltage balance once it has been identified between various sets of switching status.

However, this problem can be effectively mitigated by changed switching, as presented in [16]–[18]. The converter is still sensitive to temporary errors without a feedback controller which affect the balance of the condenser voltage. A hybrid space vector (SVM) modulation is given in [16]. To cover the maximum spectrum of the index modulation, two modulation techniques are combined. On the other hand, it is important to add independent sensors and control units, which can handle the calculation required. Therefore, the system costs are raised and reliability is reduced. Similar balancing strategies based on adjusted modulation are also implemented in[17] and[18] which also suffer the same downside when moreinsulated sensor voltage and control loops are included.

In the event of a modified modulation technique additional control components (active/passive switches, condensers and/or inductors) should not be used. The solution was thus deemed to be ideal. If a wide range of operational and defect tolerances are to be reached, however, additional sensors and control loops must be added. The capacity of the condenser to control and equalize the voltages is further limited by the multi-level transducer itself. The voltage balance of the condensers in the MLI is also achieved, as shown in Figure, when the input power source of an additional circuit is applied to the MLI (baiter batteries linked to the EV bidirectional converter). 1 As introduced in [19], the additional circuit can be an active circuit. Two power switches, three diodes and two inductors are connected by two captors on the voltage balance circuits implemented in [19]. it suffers the same problems as additional components and controls are required to increase the complexity of the system. It also does not restrict operation to engine use only as defined in [19]. In [21] a new multi-level converter is implemented based on the same concept which does not allow the 4-quadrant drive even if the condenser voltage imbalance in MMC is solved.

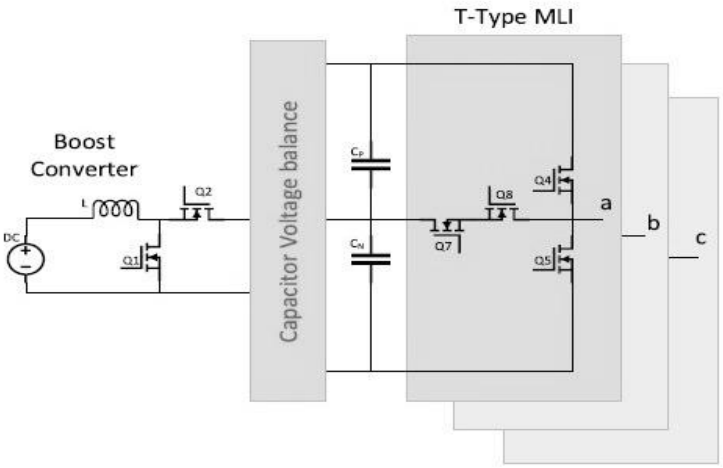

Fig. 1 Conventional configuration of a dc–dc converter connected to a voltage balancing circuit before connected to the T-type MLI.

In [22] three active switches and two inductors control condenser pressures in order to balance the tension between three input condensers. These modules are fitted with two buck converters to control the voltages of the condensers. This circuit requires additional feedback and control loops for the purpose of such configuration. In addition, the inducers are less preferable compared with the condenser-based voltage balance circuit.

Initially introduced in [23]–[25], the multi-level dc–dco booster converter can only work like a unidirectional boost converter, which makes it impractical for electric powertrains, particularly EV applications. The design was then modified by replacing the CM clamping diodes with two active

power switches. As shown in figure, these two switches operate by the synchronous boost converter. 2 Reservations are also made on simplifying the original contracture and the control signal quantity. Therefore, a bidirectional operation is possible when the input voltage is increased in engine mode and the combined condenser voltage is blown into regenerative mode. The condenser sizing of the converter is then discussed. Finally, both simulation models have tested the validity of the proposed configuration.

II. T-STYLE TOPOLOGY

Fig.2 demonstrates the general T-style simple circuit topology. Basically, it consists of a two-way switch in series, which blocks the DC link voltage from either side of the DC (combined with the antiparallel diode). The commands (Q2,Q4) are used in (+) Vdc/2 generation, and switches (Q1,Q3) are used to generate (-) Vdc/2 complimentary.

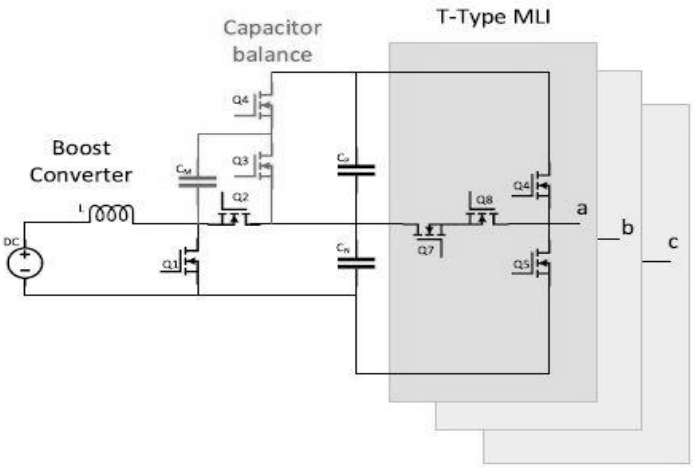

Fig.2 Proposed configuration of a multilevel bidirectional dc–dc converter connected to the T-type MLI.

Typical MLI topologies such as DCMLI, FCMLI and CHBMLI were found for many applications but are highly complex in literature. The system includes large gateways and level shifting circuits which can increase cost and require separate circuit DC communication sources. In the topology suggested for 3-phase trunk circuits, various SVPWM methods use the reverse-voltage DC voltage technology previously proposed in[3]. The most advanced inverter control technology is SVPWM. When a waveform is intersected by a high-frequency triangular carrier, high frequency SVPWM systems for MLIs are the most effective. The document shows that in relation to their part number and less THD, the solution proposed is better than standard, multi-level inverters. Using a two-way power transfer to the DC link blocks dc voltage (half). Two MOSFETs, including parallel diodes, are shown in figure 2 for devices with reduced voltage rates. The center switch displays a very low lead loss switch, and two units can be connected in series due to the reduced blocking voltage. No unit is connected to block the complete Vdc in one sequence, unlike the topology of DCMLI 5. Normally transformations from positive (P) to negative (N) dc voltage are removed from DCMLI topology. Since it is appropriate to block the irregular voltage, when the two MOSFETS are simultaneously switched off by connected series. In topology, this undesirable effect cannot occur. This technique is

not suitable in a low-tension application so it is important to introduce an adapted relation between the MOSFET series. The MLI with DC inputs is a three-stage 5-stage MLI.

III. PROPOSED SYSTEM CONFIGURATION

The dc power supply is usually connected to the bi-directional dc-dc converter which controls DC bus voltage from the point of view of the system propeller. A dc-dc converter output and the MLI input are voltage balancing circuits. The input dc source is connected to a bidirectional MDC-DC converter in the proposed configuration as shown in Fig2. The divided condensers supply the voltages needed for the ac voltage of the MLI. A CM condenser is added to an intermediate storage of electricity by the two-way converter dc–dc. The excess power from the higher CP condenser is transferred to the lowest CN, vice versa. The converter therefore achieves a normal voltage equilibrium between CP and CN without any input or added control circuit.

While multilevel converters use two additional switches and a condenser that affect train costs and size, it is preferable to add two voltage gains for the same service time in the conventional boost converter. The reverse blocking tension displayed by one of the power switches is not increased. The multilevel dc-dc conversion system therefore uses the power switches with half Vb for the same output tension and operates at half D in contrast to the normal boost.

IV. CIRCUIT OPERATION

In mechanical state (1) step-up and (2) bucking mode, the process for the proposed Converter configuration is divided into two separate modes (renewable). It must be noted that in the continuously moving mode the boost converter works where the mean induction current exceeds the decline. The image. The picture. 3 (a) and (b) showing the current flow from dc to the lower condenser CN to the CM and the maximum condenser CP during the TS-conversion era. In this situation, MLI works in a typical state where each condenser, CN and CP, is equivalent in power. Therefore, the boost converter always pushes the power to the CN transmitted to CP through CM. Image. Fig. The first condition of DTS > t >0 will appear in 3 (a) The Shuttle
Q1 is ON and Q2 is OFF, which allows an increase of iL inductor current. The middle CM condenser binds to CN simultaneously with Q3 ON and Q 4 OFF. CN has a higher VCN voltage than CM voltage VCM since it is directly connected to the boost converter. As the arrows illustrate, the output is transmitted from CN to CM. Fig demonstrates the second condition. 3(b) TS > t> DTS in which, while Q2 is ON, Q1 is OFF. The inductor is loaded through Q2 to CN, thereby increasing its voltage of the VCN.
DTS >t 0 is initially used for the Q2 and Q4 mode during Q1 and Q3. CN transfers the recovery power to the DC source and the L inductor and the Cin condenser are supplied with power. In the meantime, since VCP is higher than VCM, CP loads CM over Q4.

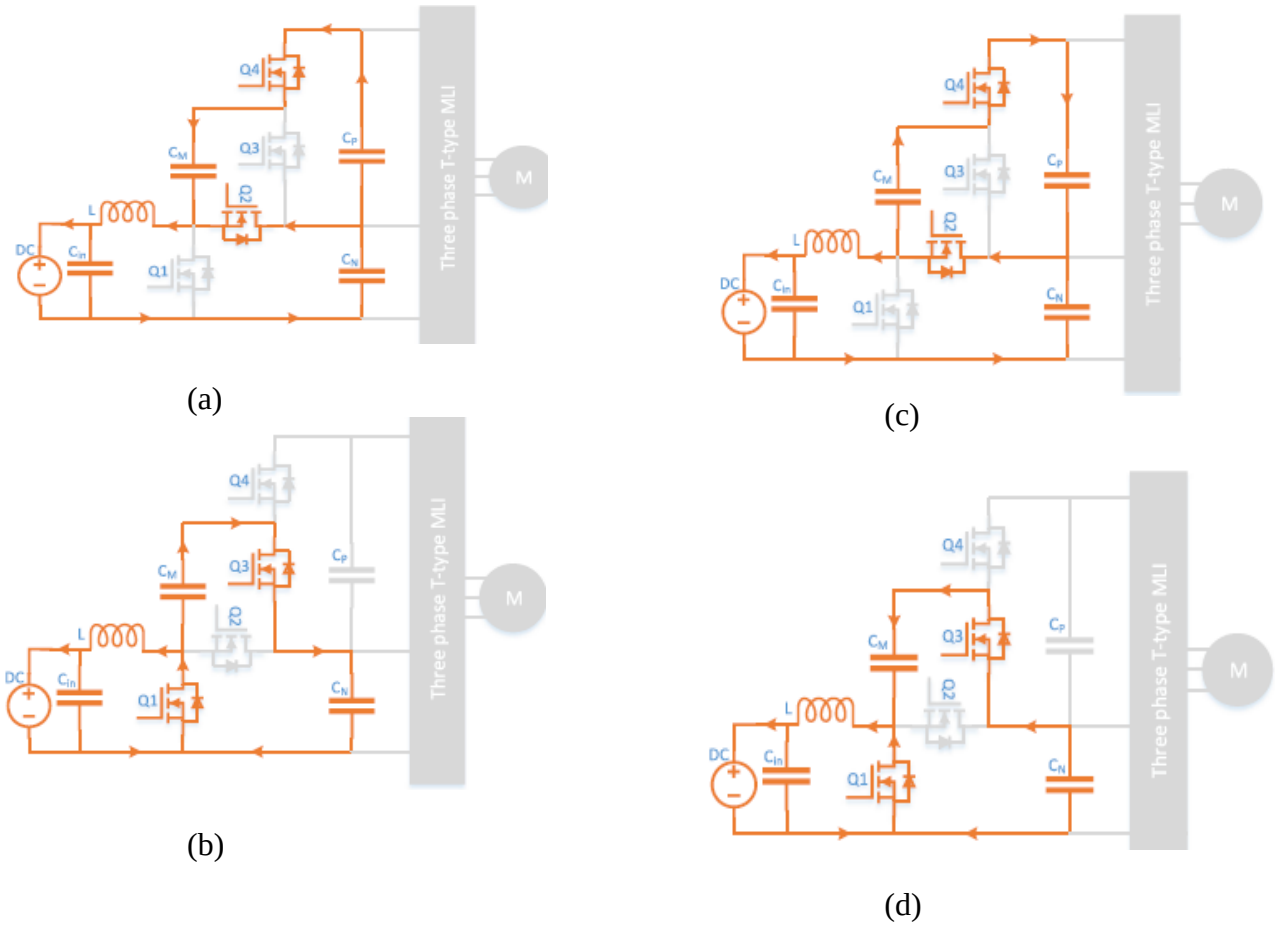

Fig. 4 Operation of the proposed configuration in bucking mode in breaking (regenerative) drive mode.

However, as shown in Figure, it is possible to reverse the flow of power between CN, CM and CP. 4(c) and 4(c) and (d). When the voltage is above CN (VCN>VCP), for example. In this scenario, the power is transferred from CN to CM at TS > t > DTS, as shown in Fig.4 In this case (d). Therefore, if CM is attached to the CP, Q4 is loaded, and a loop is repeated as shown in Fig.4.(c). The converter can now be found to act as a bidirectional converter rather than to operate as a unidirectional converter. The dc-dc converter loads the lower condenser CN at the output voltage VCN = Vdc/ (1 − D) in regular operation (in boost mode). CM is an intermediate storage device that loads CN and loads the CP at the same voltage during the same cycle. CM is charged from CP in bucking mode and then loads CN, thus guaranteeing reverse power voltage balance. The balance of the condenser and the dc bus voltage is therefore maintained between VCP + VCN = 2 Vdc/(1 − D) (in boosting mode). Vrev=VCN = VCP=VDC/(1 – D), with each of the power switches Q1, Q2, Q3, and Q4, is associated to the reverse voltage of this device.The power output of the dc bus is = 2Vdc/(1 − D). Image. Fig. 4(e) displays theoretical waveforms of the condenser voltages in a constant state relative to Q1 Gating signal, which further illustrated the voltage balance of the condenser loading/unloading.

Finally, it must be noted that when two condensers are in contact with the voltage at a different level, an inrush current spike is produced. Thus, in series with the middle condenser CM, a small inductance is added to limit such current. In this case an inductor of 1 μH is adequate to restrict the inrush current to approximately 50 kHz for a load nominal current.

V. CAPACITOR DESIGN

Image. 5 (a)–c) display a T-type MLI output ac voltage generation in single-phase (phase a) at the charge terminal and link a positive half-cycle to a CP condenser by Q4, as shown in figure. 5 5 (a). The load is linked to CN through Q5, as shown in figure, in the negative half cycle. Quarter Fifth (b). As shown in Figure 3, the level of zero-tension is created by the bidirectional switch Q7 & Q8.

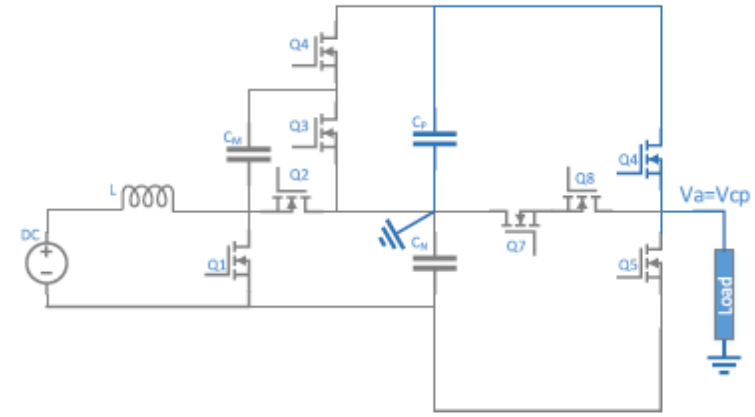

(a)

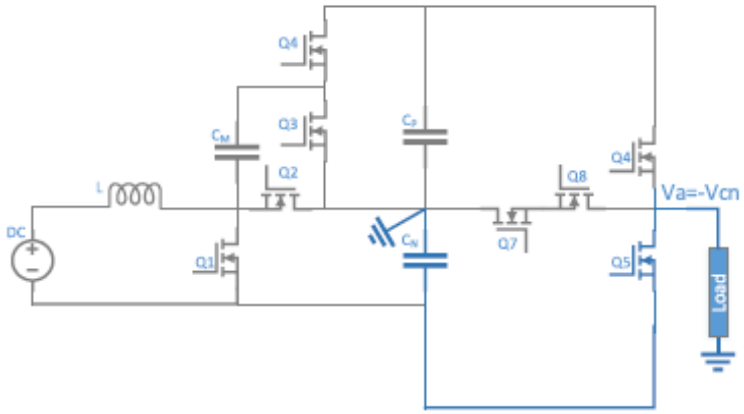

(b)

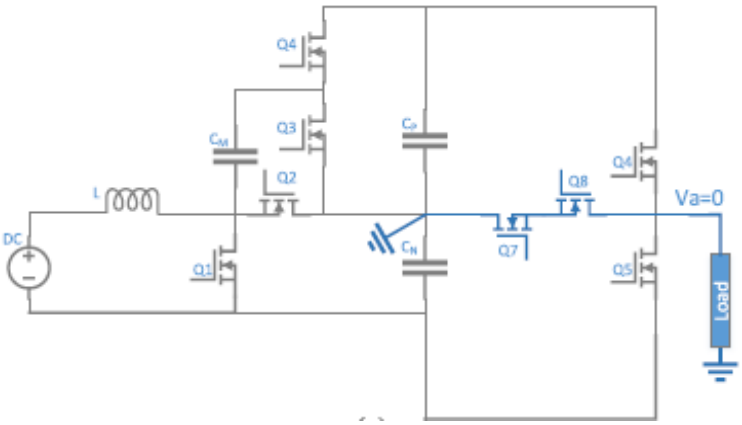

(c)

Fig. 5.Switching states of the T-type multilevel converter

Capacity of CP and CN should therefore be sufficiently high to produce load rated power and keep its voltage on a minimal level. Capacity can be measured accordingly:

$$C = \frac{\mathrm{P}}{2*\pi*f*dv*V^2} \qquad (1)$$

Where P charges power, V loads voltage, the wave is dv and the charge changes frequency is f.

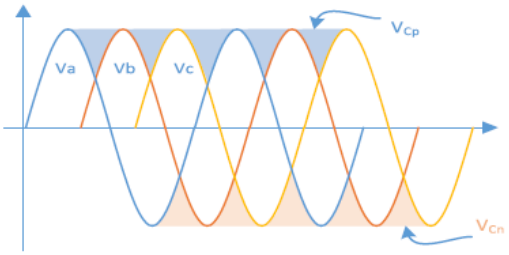

Fig. 6 Compensate for the variation in the load power at low frequency *f* = 180 Hz (for 60 Hz system) in T-type MLI.

The condensers are designed to compensate for a voltage shift at low frequency f=180 Hz (for 60 Hz), with tension = 10%, contrary to the T-type MLI inverter for three phase voltage sources.
The voltage of both the (CP and CN)VCP (VCN) and middle condenser CM as shown in Fig) is balanced in the proposed configuration. 4 That means the voltage across all condensers is equalized in every Tsof switching time, VCN =VCM =VCP. Therefore, all condenser tension wafers are in phase and the output voltage waft is increased in V bus dc.

Accordingly, on the basis of the design of the two-way HF converter to fill the switched voltage, each capacitor has its ability, thereby leading to slightly less condensing capacity. Therefore, electrolytic condensers connected to this MLI that usually have a considerably longer life and stabilized performance can be replaced [27].
The voltages of the DC bus or unwanted harmonics in the driving train do not affect this. Equation (2) is used for measuring per HF boost converter's minimum required capacitance as follows:

$$C = \frac{\mathrm{VD}}{2\mathrm{f_s}\,\mathrm{dv}\ \mathrm{R}} \qquad (2)$$

If V is the Dc V bus, D is the nominal boost for the operating cycle, fs is the frequencies for switching, dv is the voltage ribbed permissible in voltage (V) and R is the corresponding ohmic power. Therefore, the required capacity of the film condensers is 15 µF, which is available on the markets according to this example (with a 200 V tension input).

However, the reverse is expressed in its input current due to the corrections of the low-frequency wave from the boost input (inductor current). Therefore attention is needed to avoid the operating of a converter on a discontinuous drive mode when the induction current is above 0 A if the value of the input inductors and condensers is constructed according to maximum low frequency rib. In continuous driving for each boost converter, the following equation indicates the limit:

$$\frac{2\mathrm{Lf_s}}{\mathrm{R_{critical}}} > \mathrm{D}(1-\mathrm{D})^2 \qquad (3)$$

If L is the inductance value of the inductor converter and R is the respective output resistance which causes the boost to drive discontinuously.

VI. PROPOSED CONTROL SYSTEM

Fig 8. Displays SVPWM control system block diagram used in T type multi-level inverter control. Block diagram.

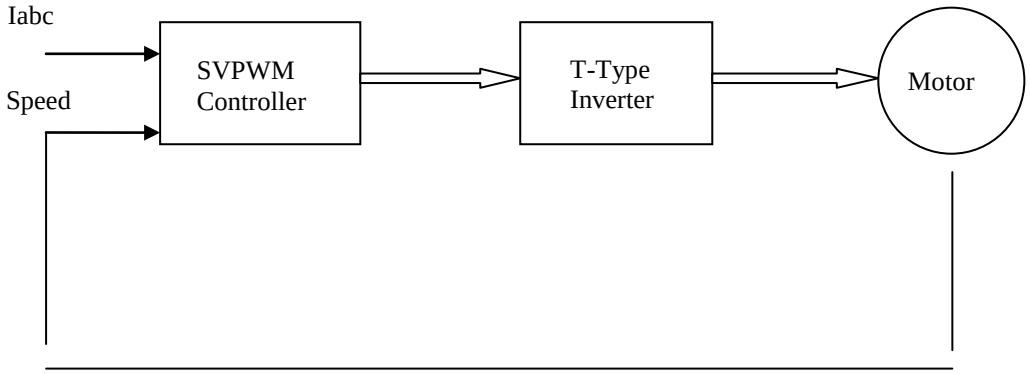

Fig 8 Block diagram of SVPWM control

The generation module for Space Vector PWM takes commands to the modulation index and generates the right wave for every PWM loop. This segment explains how the SVPWM module functions and settings.

A two-tier three phase inverter with a dc connection configuration can produce an inverter output voltage under 8 possible switching conditions. Space vectors (active vectors, non-voltages V7 and V8) in the Vector space aircraft conduct all inverter switching conditions (Figure: space vector diagram). Each vector is 2/3 Vdc in magnitude (V1-V6) (dc bus voltage).

By the following equation (linear range), the inverter is able to reach the fundamental line-to-line Rms voltage (Vline):

$$V_{line} = U_{mag} * \text{Mod\_Scl} * V_{dc}/\sqrt{6}/2^{25} \qquad (4)$$

Where there is a voltage dc bus (Vdc)

The linear spectrum of maximal possible modulation (Umag L) is:

$$U_{mag\_L} = 2^{25} * \sqrt{3}/\text{Mod\_Scl} \qquad (5)$$

The modulation over Umag>Umag L takes place. Over modulation. This is the state under which the voltage rises beyond the boundary of the hexagon. In these circumstances, under these circumstances, The PWM-algorithm Spacious Vector can resize the tension vector to suit inside Hexagon. The voltage vector size within the hexagon is lowered but the angle of phase (AD) remains constant.The transmission gain of the PWM modulator in the over-modulation area is reduced and not linear.

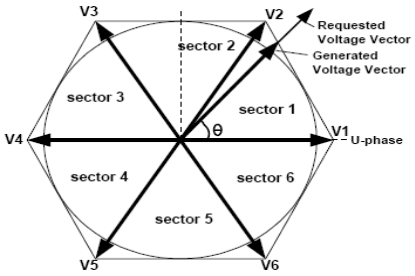

Fig: 9 Voltage Vector Rescaling

The figures above show the wavelength of a PWM vector in the space vector sector I

VII. SIMULATION RESULTS

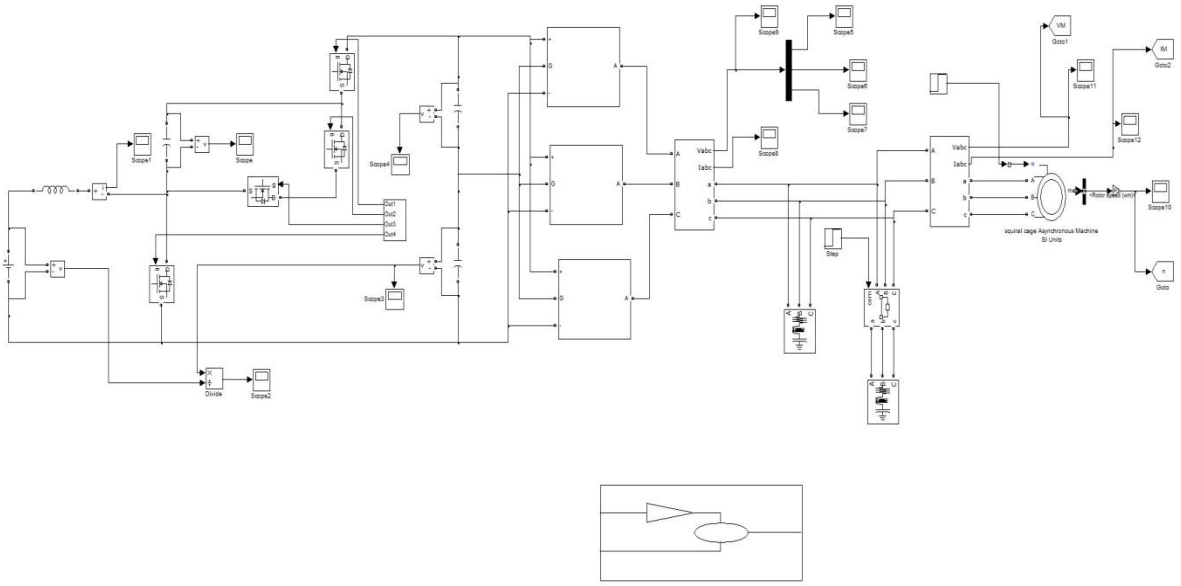

Fig12. Simulation circuit diagram of proposed system

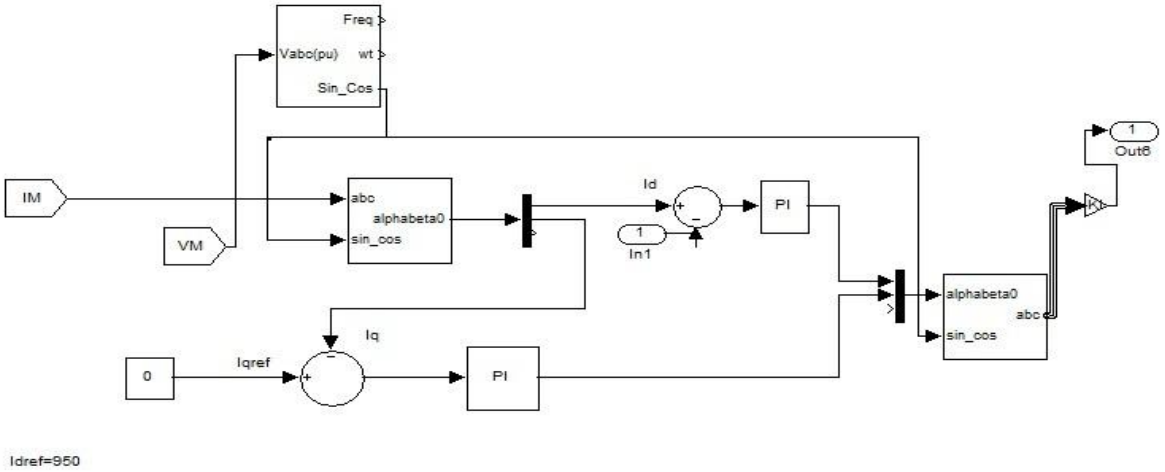

Fig.13 SVPWM controller subsystem

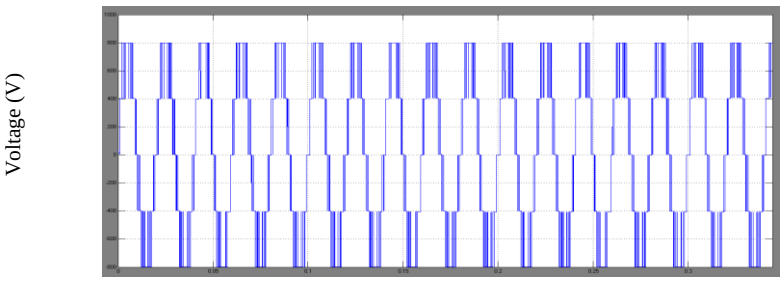

(a)Vab

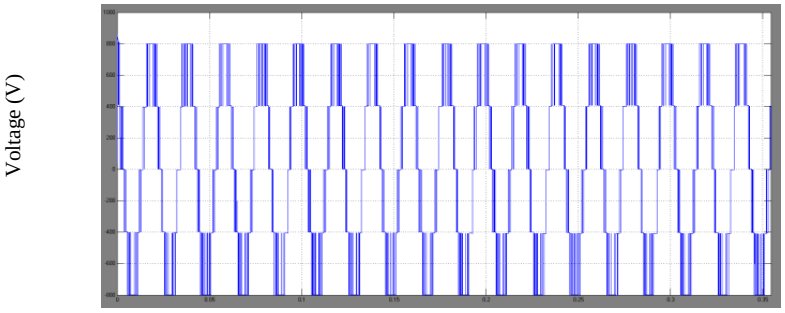

(b)Vbc

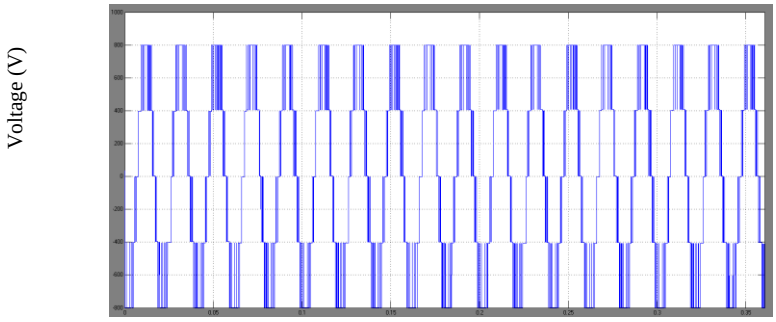

(c)Vca

Fig.14 Three-phase line-to-line output voltage.

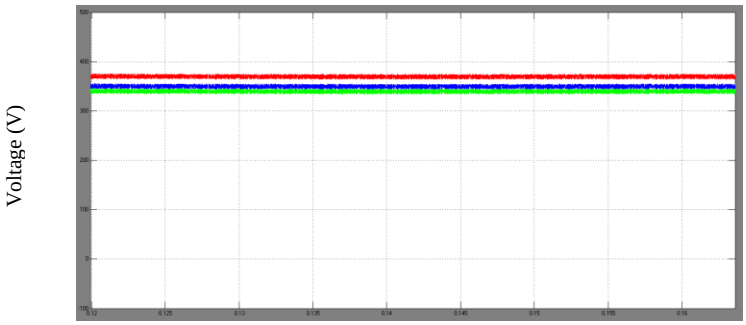

(a) LF ripple on Cp,Cn,Cm voltages corresponds to three-phase output power(Red colour represents-Cp, Blue colour represents-Cn, Green colour represents-Cm)

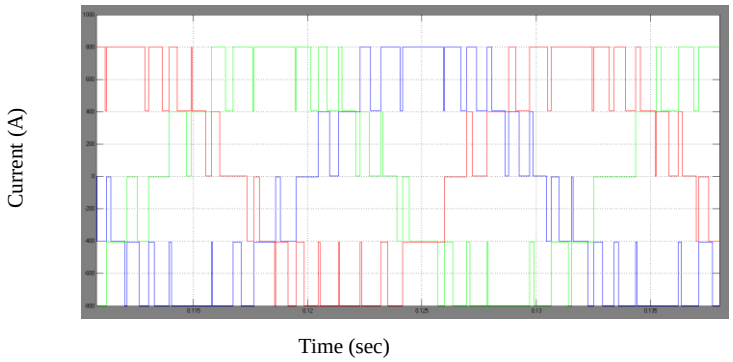

(b)Three-phase output voltage (Vabc)

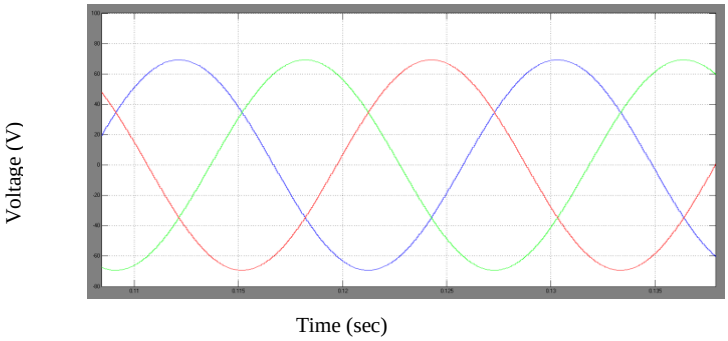

(c)Three-phase output current(Iabc)

Fig. 15 Low-frequency ripple on capacitor voltages *V*CN,*V*CM, and *V*CP.

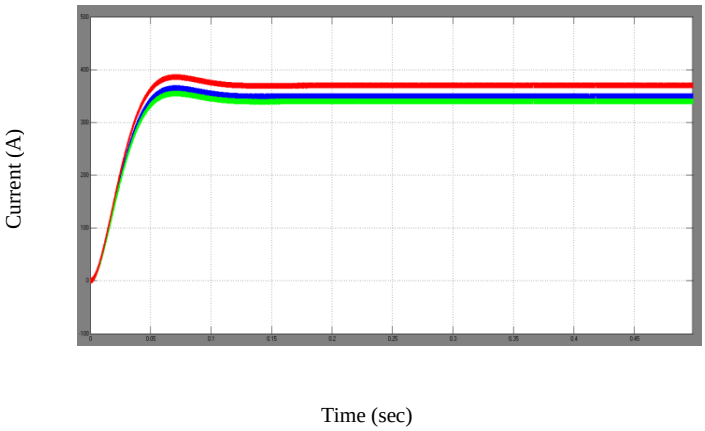

Fig.16. Capacitor voltage at steady state (Red colour represents-Cp, Blue colour represents-Cn , Green colour represents-Cm)

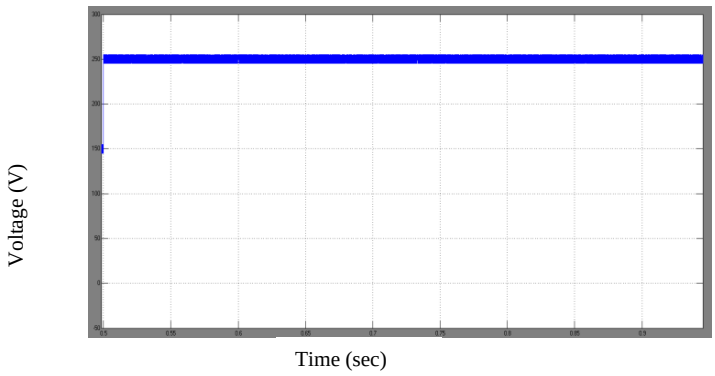

Fig.17 Inductor current at motoring mode.

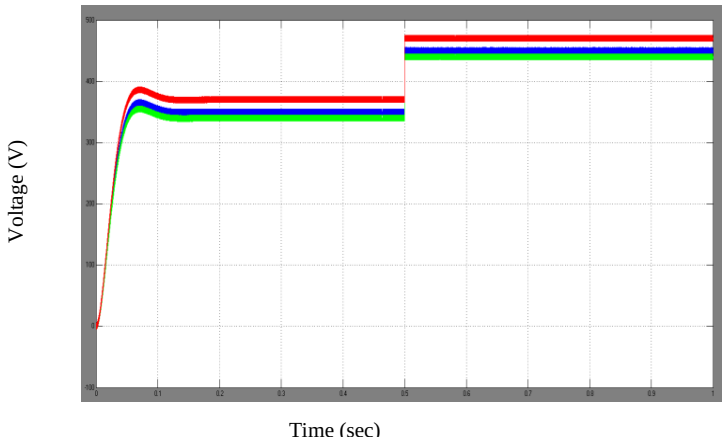

(a) Capacitor voltages (Red colour represents-Cp, Blue colour represents-Cn , Green colour represents-Cm)

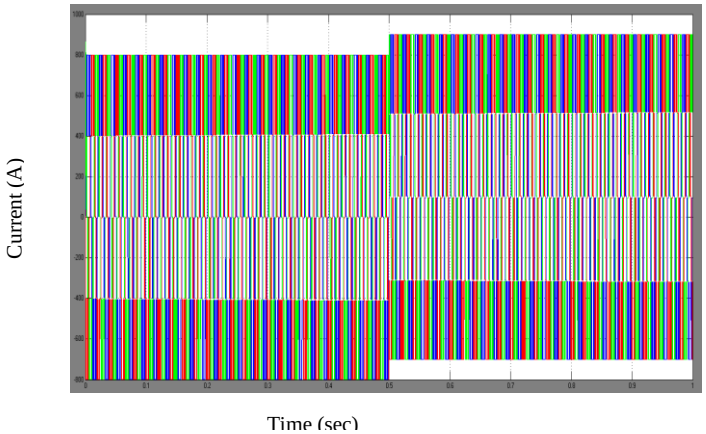

(b) Three-phase output voltage (Vabc)

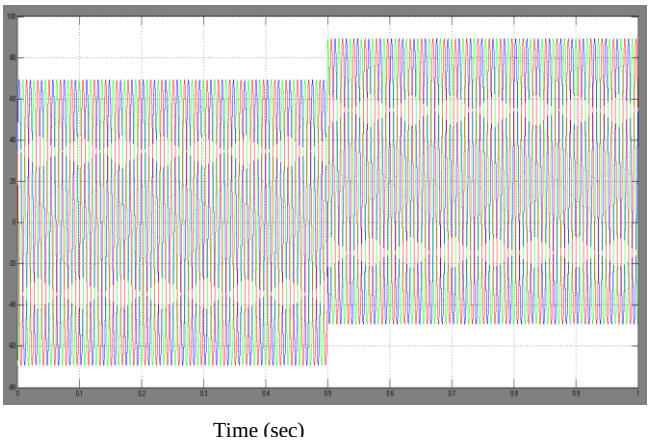

(c) Three phase output current (Iabc)

Fig.18 Voltage of the converter's capacitor at step change and fault condition. (a) Step change in the dc link voltage reference from 275 to 375 V at t = 0.05 s.

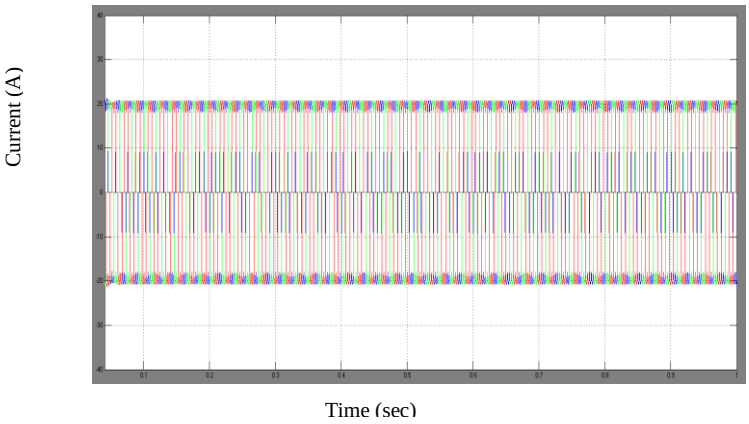

Fig19. Motor current in regenerative mode

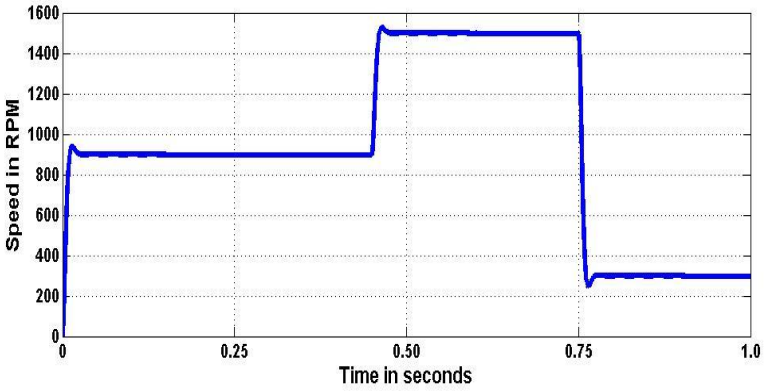

Fig.20 Speed of the motor.

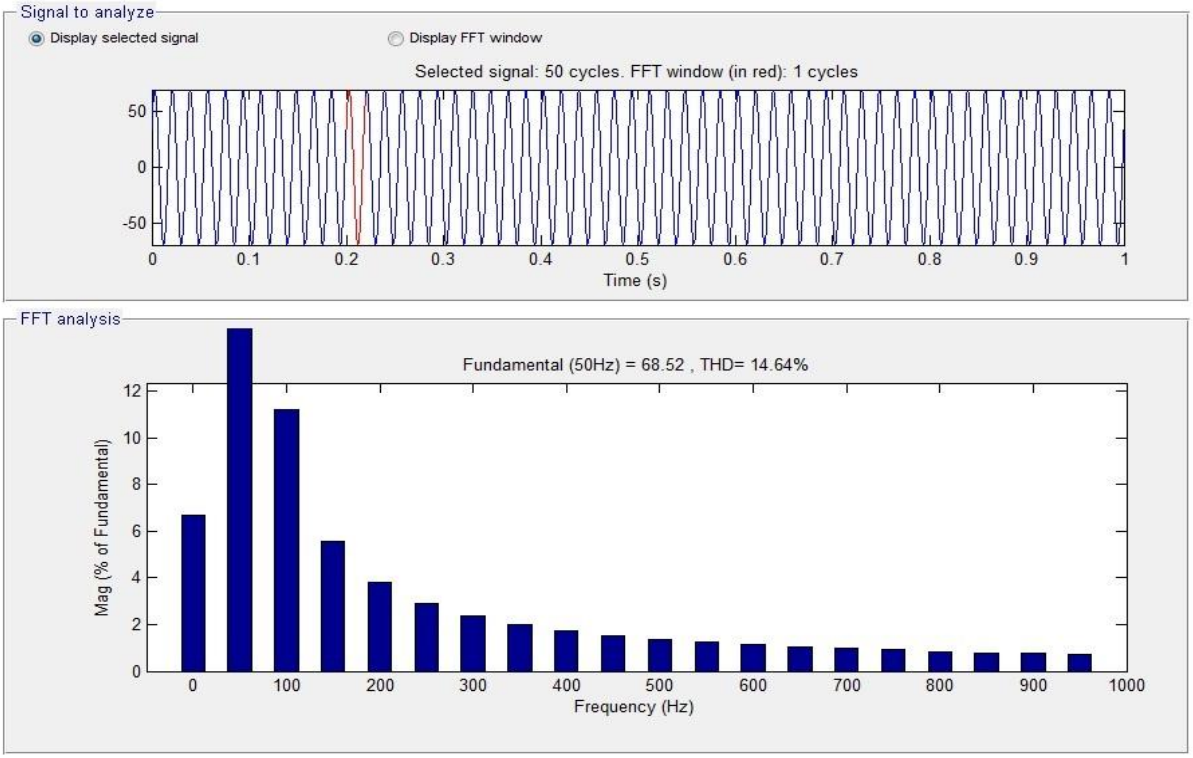

Fig.21 THD of Inverter output current is 14.64% with SVPWM controller

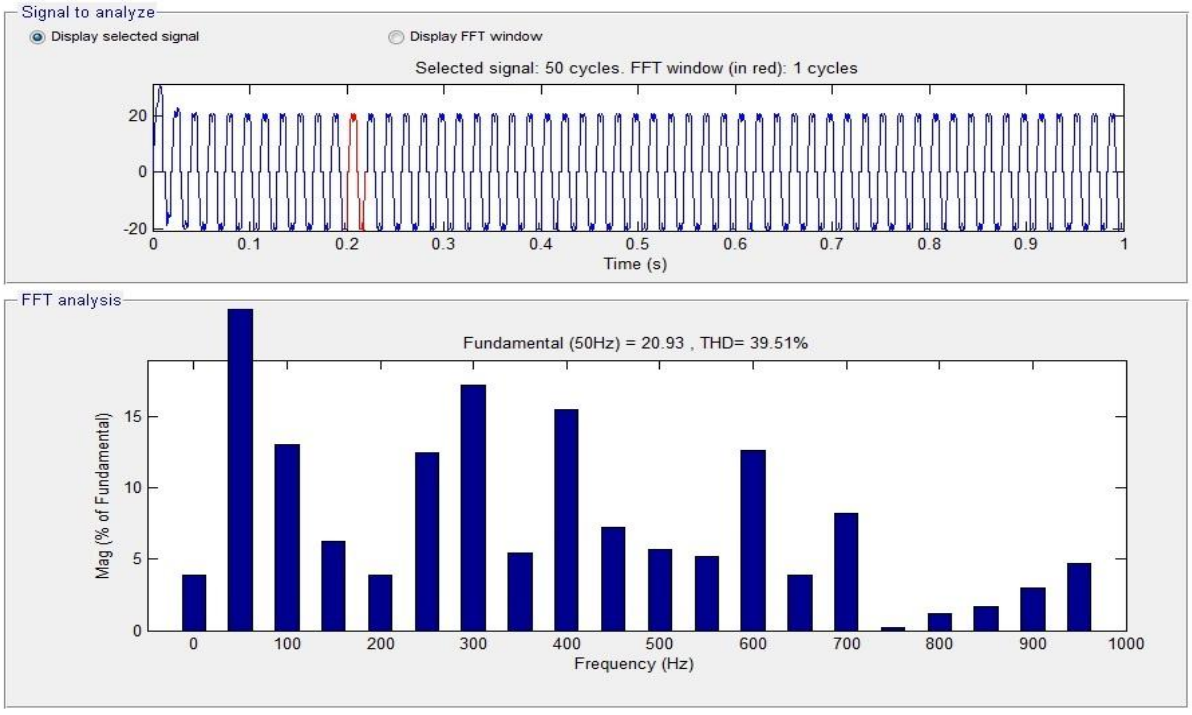

Fig.22 THD of motor current is 39.51% with SVPWM controller.

COMPARISON TABLE

Control scheme	**THD% of Inverter output current**	**THD% of motor current**
SPWM Control scheme	**23.79%**	**55.62%**
SVPWM Control scheme	**14.64%**	**39.51%**

VIII. CONCLUSION

This article contains a new addition to the T-type MLI based on SVPWM with an updated bi-directional dc-dc multilevel EV converter. Although the T-Type MLI has more power, switches produce more voltage at half the voltage reverse than traditional inverters with power switches. But the converter needs to be set up in a traditional dc-dc converter to handle the maximum power of the dc bus. In addition, it integrates a voltage equilibrium circuit or unique switching configuration with feedback and control loops to maintain a dc condenser tension balance. Depending on the input stage of dc-dc, the condensers are not designed to rupture the bass line up to 180 Hz. The required capacitance is reduced from several hundred condensers μF to 10 μF, enabling film condensers to be replaced by electrolyte. The proposed converter doesn't affect its capacity in step-up and step-down mode to power the electrostatic motor. In addition, both power switch and condenser-rated voltage have a maximum reverse voltage of about half the maximum ac output Voltage, decreasing voltage voltage and making side-by-side dc/dc performance swits similar to those on the side of T-type MLI. This compares the results and addresses the advantages of the design proposed over the traditional market structure (THD). The over-shooting effect of condensers Vcm,VcnandVcp voltages often decreases from 10 percent to 5 percent. This leads to high reliability and higher performance by reducing these factors using the SVPWM technique and using speed controls.

REFERENCES

[1] Y. Attia, A. Abdelrahman, M. Hamouda, and M. Youssef, “SiC devices performance overview in EV DC/DC converter: A case study in a Nissan Leaf,” in Proc. IEEE Trans. Electrification Conf. Expo, Asia - Pacific, 2016, pp. 214–219.
[2] K. Tian, B. Wu, M. Narimani, D. Xu, Z. Cheng and N. Reza Zargari, "A Capacitor Voltage-Balancing Method for Nested Neutral Point Clamped (NNPC) Inverter," in IEEE Transactions on Power Electronics, vol. 31, no. 3, March 2016, pp. 2575-2583.
[3] G. S. Lakshmi, "Performance Analysis of Multi-Level Diode-Clamped Inverter fed IPMSM Drive for Electric Vehicles," 2018 IEEE Innovative Smart Grid Technologies - Asia (ISGT Asia), 2018, pp. 54-61.
[4]A survey on space-vector pulse width modulation for multilevel inverters by Q.M. Attique, Y. Li, and K.Wang, published in CPSS Trans. Power Electron. Appl., vol. 2, no. 3, Sep. 2017, pp. 226–236.

[5] V. Fernão Pires, D. M. Sousa and J. F. Martins, "Controlling a grid-connected T-type three level inverter system using a sliding mode approach," 2014 IEEE 23rd International Symposium on Industrial Electronics (ISIE), 2014, pp. 2002-2007.
[6] H. Chen, P. Wu, C. Lee, C. Wang, C. Yang and P. Cheng, "Zero-Sequence Voltage Injection for DC Capacitor Voltage Balancing Control of the Star-Connected Cascaded H-Bridge PWM Converter Under Unbalanced Grid," in IEEE Transactions on Industry Applications, vol. 51, no. 6, , Nov.-Dec. 2015, pp. 4584-4594.
[7] G. E. Valderrama, G. V. Guzman, E. I. Pool-Mazún, P. R. Martinez-Rodriguez, M. J. Lopez-Sanchez and J. M. S. Zuñiga, "A Single-Phase Asymmetrical T-Type Five-Level Transformerless PV Inverter," in IEEE Journal of Emerging and Selected Topics in Power Electronics, vol. 6, no. 1,March 2018, pp. 140-150.
[8]M. Khazraei, H. Sepahvand, K. A. Corzine and M. Ferdowsi, "Active Capacitor Voltage Balancing in Single-Phase Flying-Capacitor Multilevel Power Converters," in IEEE Transactions on Industrial Electronics, vol. 59, no. 2, Feb. 2012, pp. 769-778.
[9]A. K. Verma, B. Singh and D. T. Shahani, "Grid to vehicle and vehicle to grid energy transfer using single-phase bidirectional AC-DC converter and bidirectional DC-DC converter," 2011 International Conference on Energy, Automation and Signal, 2011, pp. 1-5.
[10] Z. Tao and L. Li, "Control loop design and bidirectional control strategy of a bidirectional DC/DC converter," IECON 2017 - 43rd Annual Conference of the IEEE Industrial Electronics Society, 2017, pp. 5720-5725.
[11]V. Jeyakarthikha and K. R. Vairamani, "Multiport bidirectional dc-dc converter for energy storage applications," 2014 International Conference on Circuits, Power and Computing Technologies [ICCPCT-2014], 2014, pp. 411-417.
[12] P. He and A. Khaligh, "Comprehensive Analyses and Comparison of 1 kW Isolated DC–DC Converters for Bidirectional EV Charging Systems," in IEEE Transactions on Transportation Electrification, vol. 3, no. 1,March 2017, pp. 147-156.
[13] K. Yoo and J. Lee, "A 10-kW Two-Stage Isolated/Bidirectional DC/DC Converter With Hybrid Switching Technique," in IEEE Transactions on Industrial Electronics, vol. 60, no. 6, June 2013, pp. 2205-2213.
[14] Y. Lee, A. Khaligh and A. Emadi, "Advanced Integrated Bidirectional AC/DC and DC/DC Converter for Plug-In Hybrid Electric Vehicles," in IEEE Transactions on Vehicular Technology, vol. 58, no. 8, Oct. 2009, pp. 3970-3980.
[15] M. A. Khan, A. Ahmed, I. Husain, Y. Sozer and M. Badawy, "Performance Analysis of Bidirectional DC–DC Converters for Electric Vehicles," in IEEE Transactions on Industry Applications, vol. 51, no. 4, , July-Aug. 2015, pp. 3442-3452.
[16] N. Nguyen, T. Tu Nguyen and H. Lee, "A Reduced Switching Loss PWM Strategy to Eliminate Common-Mode Voltage in Multilevel Inverters," in IEEE Transactions on Power Electronics, vol. 30, no. 10, Oct. 2015, pp. 5425-5438.
[17] N. A. Rahim, M. F. M. Elias and W. P. Hew, "Transistor-Clamped H-Bridge Based Cascaded Multilevel Inverter With New Method of Capacitor Voltage Balancing," in IEEE Transactions on Industrial Electronics, vol. 60, no. 8, Aug. 2013, pp. 2943-2956.
[18]Z. Cheng and B. Wu, "A Novel Switching Sequence Design for Five-Level NPC/H-Bridge Inverters With Improved Output Voltage Spectrum and Minimized Device Switching Frequency," in IEEE Transactions on Power Electronics, vol. 22, no. 6, Nov. 2007, pp. 2138-2145.
[19] S. Brueske and F. W. Fuchs, "Efficiency optimisation of a neutral point clamped inverter for electric vehicles by means of a variable DC input voltage and different power semiconductors," 2014 16th European Conference on Power Electronics and Applications, 2014, pp. 1-10.
[20] A. Choudhury, P. Pillay and S. S. Williamson, "A hybrid-PWM based DC-link voltage balancing algorithm for a 3-level neutral-point-clamped (NPC) DC/AC traction inverter drive," 2015 IEEE Applied Power Electronics Conference and Exposition (APEC), 2015, pp. 1347-1352.

[21] Dong-Ho Yu, Jung-Hyo Lee, Se-Chun Kim, Yong-Seok Lee, C. Won and Y. Jung, "Auxiliary switch control of bi-directional soft switching DC/DC converter for EV," Proceedings of The 7th International Power Electronics and Motion Control Conference, 2012, pp. 854-858.
[22] B. Kim, M. Kim and S. Choi, "A reduced component count single-stage electrolytic capacitor-less battery charger with sinusoidal charging," 2017 IEEE 3rd International Future Energy Electronics Conference and ECCE Asia (IFEEC 2017 - ECCE Asia), 2017, pp. 242-246.
[23] B. Koushki, P. Jain and A. Bakhshai, "An Electrolytic capacitor-less bi-directional EV-Charger with 6 switches," IECON 2016 - 42nd Annual Conference of the IEEE Industrial Electronics Society, 2016, pp. 3229-3234.
[24] J. A. Mane and A. M. Jain, "Design, modelling and control of bidirectional DC-DC converter (for EV)," 2015 International Conference on Emerging Research in Electronics, Computer Science and Technology (ICERECT), 2015, pp. 294-297.
[25] A. S.Abdelrahman, K. S. Algarny, andM. Z.Youssef, “Optimal gear ratios selection for a nissan leaf: A case study of InGear transmission system,” Proc. IEEE Energy Convers. Congr. Expo., 2017, pp. 2079–2085.